ICIC Express Letters
Part B: Applications
Volume **7**, Number **1**, January **2016**

ICIC International ©2016 ISSN 2185-2766
pp. 105–110

ENHANCEMENT OF BGA-VOID DEFECT DETECTION IN POOR CONTRAST X-RAY IMAGES USING CONFORMAL MAPPING

Somchai Nuanprasert[1], Khiy Wei Lee[2,3], Ali Hassan Mohamed Murid[2,3]
Sueki Baba[4] and Takashi Suzuki[1]

[1]Department of System Innovation
Osaka University
1-3 Machikaneyama-cho, Toyonaka 560-8531, Japan
{ somchai; suzuki }@sigmath.es.osaka-u.ac.jp

[2]Center for Industrial and Applied Mathematics
[3]Department of Mathematical Sciences
Faculty of Science
Universiti Teknologi Malaysia
81300 UTM Johor Bahru, Malaysia
leekhiywei@gmail.com; alihassan@utm.my

[4]BEAMSENSE Co. Ltd
2-19-16 Izumi-cho, Suita 564-0041, Japan
baba-sueki@beamsense.name

Received June 2015; accepted September 2015

Abstract. *To assure the reliability of high-density printed circuit boards (PCB) assemblies in electronic device manufacturing, the non-destructive inspection systems of ball grid array (BGA) connectors are needed. One of many challenges is to detect void defects occurring inside solder balls during reflow from 2D X-ray images. In this paper, we have presented the efficient method, which is to firstly apply the conformal mapping (CM) technique for transforming the circular domain of solder ball, i.e., our region of interest (ROI), to the rectangular domain before computing the well-known Contrast Limited Adaptive Histogram Equalization (CLAHE) algorithm, which is a block-based processing, in order to improve local contrast enhancement for the difficult case of images with poor contrast issue. Our experiments showed that the proposed method can enhance the performance of void defect detection by reducing the number of undetected voids effectively. An additional processing time due to the incorporation of CM into the void inspection system is about 3 seconds for one solder ball image with a matrix size 221 × 221.*
Keywords: Printed circuit boards (PCB), Ball grid array (BGA), X-ray image, Void detection, Local contrast enhancement, CLAHE, Conformal mapping

1. **Introduction.** With excellent efficiency in making high-density printed circuit boards (PCB), ball grid array (BGA), which is a type of surface-mount packages, has been increasingly used for integrated circuits in many electronic products. Currently, the need for higher density is on the increase; it leads to further reductions of solder ball size and spacing between pitches; consequently, the failures of solder joints assembly become more of a concern, especially, the high amount of voids may degrade the mechanical strength of the interconnection potentially causing the poor electrical conductivity in joints and affect the reliability for long-term use of electronics devices [1, 2]; therefore, many automated inspection techniques based on X-ray imaging were actively developed in previous studies [3, 4, 5, 6, 7] in order to achieve this requirement of quality control in manufacturing.

However, there are several factors which may reduce the accuracy of the inspection results, for example, occluded solder balls [3, 7], artifacts [3, 5], sizes and positions of voids [4], and particularly in difficult situations some images show very poorer contrast than

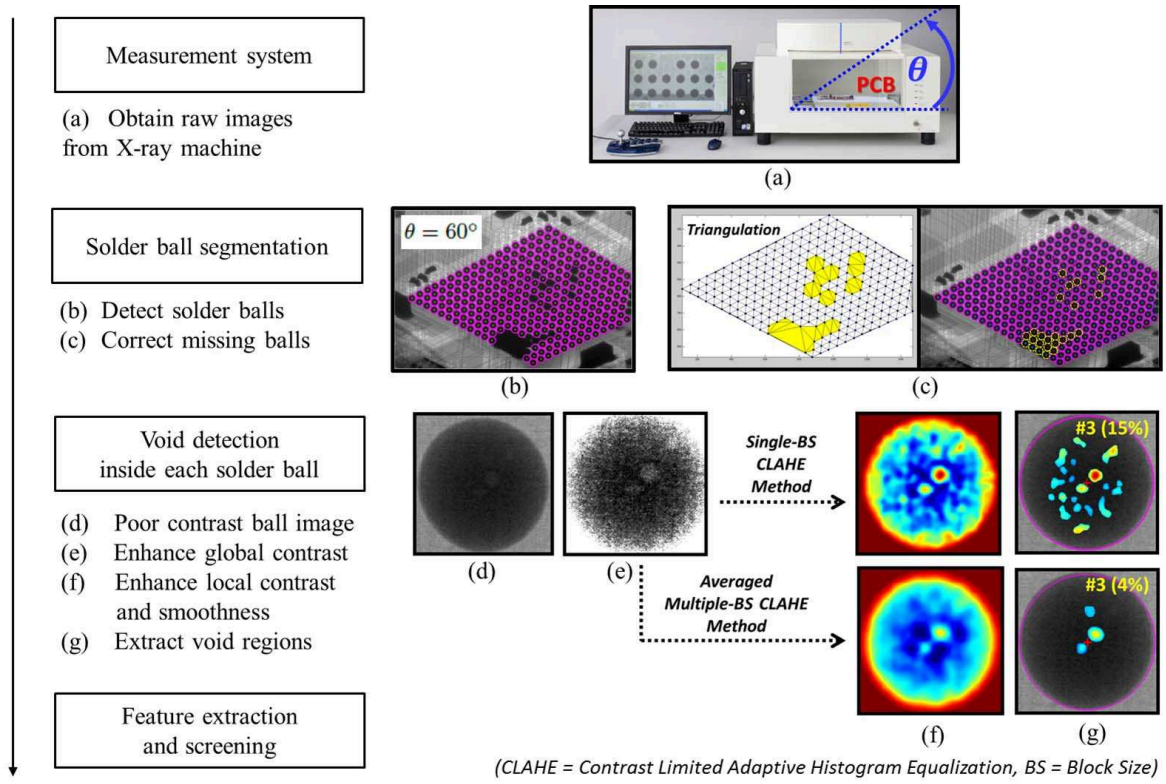

FIGURE 1. Overview of automated BGA-void defect inspection system

usually and then the local contrast enhancement algorithms, such as Contrast Limited Adaptive Histogram Equalization (CLAHE), are necessary for improving the quality in smaller scales.

To the extent of our knowledge, only our previous work in [6] focused on studying the enhancement of BGA-void detection in case of poor contrast. This work emphasized that the traditional method using CLAHE with single-block size (BS) could have the side effect of artificial fluctuations possibly detected as *false voids* causing a false alarm problem, see Figure 1 (g, upper row); the number reported in parentheses indicates the void area to solder ball area percentage ratio, which is a standard indicator of failure screening in manufacturing [1, 2]. To avoid this issue, by using a basic assumption that true void regions consistently remain in place higher than the artificial fluctuations, we thus proposed in [6] to average the multiple outputs of CLAHE over different block sizes, as shown in Figure 1 (g, lower row), which clearly helps to reduce some false voids. This finding motivated us to pursue further improvement for CLAHE implementation; in this paper, the problem of preparing a proper domain using the conformal mapping (CM) technique for CLAHE algorithm, which is a block-based processing, is presented.

The paper is organized as follows. Section 2 presents the proposed approach. In Section 3, the numerical methods of CM are reviewed and chosen to achieve the above proposal. Results are given and discussed in Section 4. Finally, Section 5 concludes the paper.

2. **The Proposed Approach.** Two essential processes are briefly described. First is the segmentation process, and it is required to segment the individual solder balls from the background images in order to get the regions of interest (ROI); some practical issues have to be considered, e.g., *occluded solder balls issue* where other board components interfere with the solder ball regions, and *solder-ball-arrangement patterns issue* when a PCB is rotated purposely for revealing some hidden void defects from different views of a solder ball. Our novel solution to these issues was developed in [7] using Hough transform, which is the well-known circle detection algorithm to locate the possible centers of solder

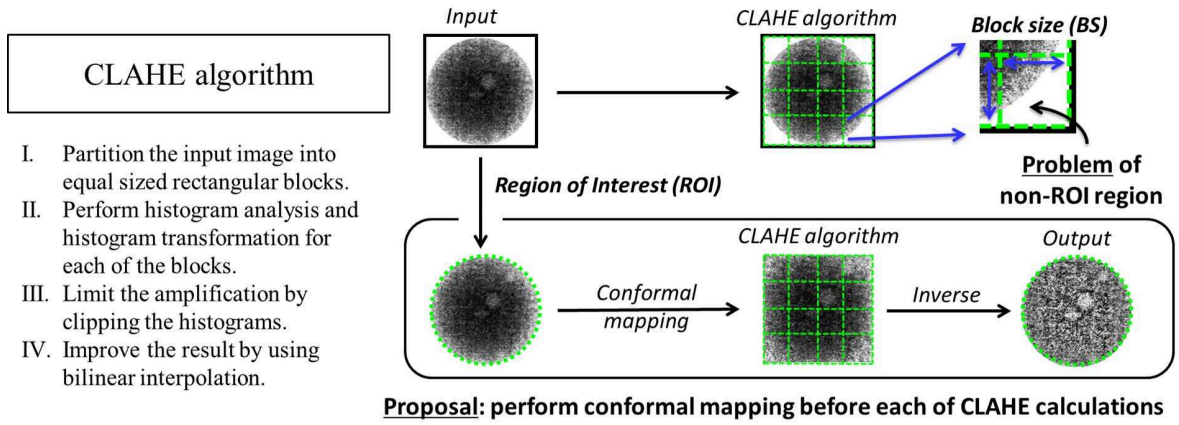

FIGURE 2. Contribution: the problem and our proposed solution

balls, applied together with the image resizing technique, as the primary detection of solder balls, as displayed in Figure 1(b). Importantly, in the next step of correcting the missing solder balls, we calculated Delaunay triangulation from all of the primary detected ball centers and performed the interpolation inside the yellow region, i.e., non-spatially periodic region to obtain the missing solder ball centers, as displayed in Figure 1(c). This proposal yields higher accuracy of segmentation and lower processing time than the conventional method in [3], which heavily relies on an image intensity distribution not geometry.

Second, it is the process of detecting voids inside each ball. Our new idea is to apply conformal mapping for transforming the circular domain of solder ball, that is our ROI obtained previously from the Hough transform, to the rectangular domain instead, which is much suitable when computing the CLAHE algorithm in order to improve the performances of local contrast enhancement and void defect detection, as shown in Figure 2.

3. **Conformal Mapping (CM).** CM is a one-to-one and onto function with non-zero derivative at every point on a domain Ω. Since it is one-to-one and onto function, no information is lost after mapping. There are several kinds of CM such as Möbius transformation, Schwarz-Christoffel mapping and Riemann mapping. Baricco et al. [8] applied CM onto face representation which improves the results obtained with other eigenface methods. Wang et al. [9] and Shi et al. [10] applied CM onto brain surface parameterization. Sangawi et al. [11] and Yunus et al. [12] have shown some results for image transformation via CM. A special theorem of CM that established the existence and uniqueness of a conformal map of any simply connected region onto a unit disk is called *Riemann mapping theorem*. Most of the methods to compute CM of bounded simply connected region rely on this theorem. The proof of this theorem can be seen in [13].

Theorem 3.1. [13] *For any bounded simply connected region Ω which is not the whole complex plane and α is an element of Ω, there exists a unique analytic function $R : \Omega \to U = \{w : |w| < 1\}$ that satisfies the conditions*

$$R(\alpha) = 0, \qquad R'(\alpha) > 0$$

and assume every value in the unit disk U exactly once.

Several methods have been proposed to compute CM of simply connected region [9, 14, 15, 16, 17, 18]. Integral equation method may give accurate solution with just a few nodes [15, 16, 19]. In integral equation method, the boundary values of the mapping function can be computed by solving integral equations. The interior values are then computed via Cauchy integral formula. Nasser and Al-Shihri [20] have employed fast multipole method

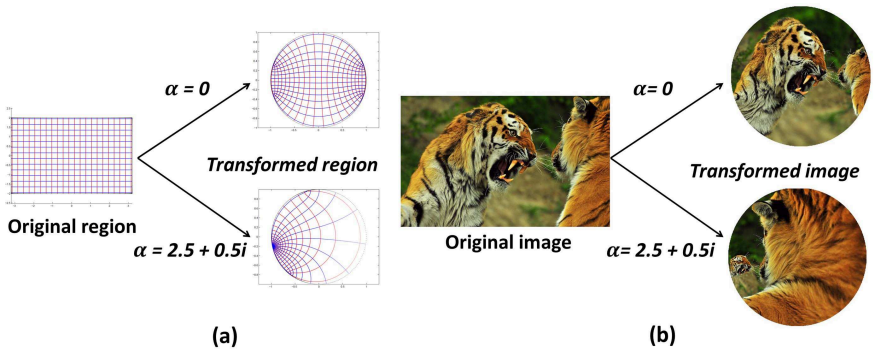

FIGURE 3. Conformal mapping from the rectangular region (a) and the image (b) onto two unit disks with $\alpha = 0$ and $\alpha = 2.5 + 0.5\mathrm{i}$

(FMM) for fast computation of CM via integral equation method. Yunus et al. [12] presented numerical CM of unbounded piecewise smooth region using the discretization by Nyström method on graded mesh.

CM of a rectangular region onto unit disk and its inverse is considered in this paper. Take t as the parameter, and discretize t using Nyström method on graded mesh (see [21] for more details), and $z(t)$ as the parameterization of the boundary of rectangular region, $R(z(t))$ as the boundary values of conformal mapping of a rectangular region to unit disk, and $\theta(t)$ as the boundary correspondence function where $\theta(t) = \arg(R(z(t)))$. In this paper, the method by Kerzman and Trummer [16] is used to compute $R(z(t))$ and $\theta'(t)$. The linear system that arised is solved by using generalized minimal residual (GMRES) method [22]. Every iteration of GMRES required matrix-vector multiplication which can be done using FMM [20]. The interior values of the mapping function and inverse function are computed using Cauchy integral formula in the form of [13]

$$R(z) = \left(\int_0^{2\pi} \frac{R(z(t))z'(t)}{z(t) - z} dt\right) \Big/ \left(\int_0^{2\pi} \frac{z'(t)}{z(t) - z} dt\right), \qquad z \in \Omega, \tag{1}$$

$$z = R^{-1}(w) = \left(\int_0^{2\pi} \frac{R(z(t))z(t)\theta'(t)}{R(z(t)) - w} dt\right) \Big/ \left(\int_0^{2\pi} \frac{R(z(t))\theta'(t)}{R(z(t)) - w} dt\right), \qquad w \in U. \tag{2}$$

The denominators in (1) and (2) both have value equal to one. This approach gives better approximation for z near the boundary of Ω [23]. Formulas (1) and (2) can be computed efficiently using FCAU MATLAB function (see [24] for more details). Figure 3(a) shows the CM of a rectangle onto unit disks with $\alpha = 0$ and $\alpha = 2.5 + 0.5\mathrm{i}$. Figure 3(b) shows the image transformation of rectangle onto the same two unit disks.

4. **Experimental Results and Discussion.** In this experiment, our objective was to evaluate the performances of void defect detection between with and without applying the conformal mapping (CM) technique and the rest conditions in all other processes were controlled; the comparison results were shown in Figure 4. Firstly, Figure 4(a) presents how we mapped from a solder ball region to its rectangular transformation before the local contrast enhancement using the averaged multiple-BS CLAHE method was calculated, and vice versa. Secondly, in Figure 4(b), we demonstrated two examples, which confirmed that the CM technique helps to increase the sensitivity of void defect detection by improving the local contrast effectively inside both solder ball regions and successfully results in the reduction of undetected cases. The overall processing time of CM stages for calculating one solder ball image with the matrix size 221×221 took around 3 seconds (on Intel Core i7-2600 3.4 GHz, 16 GB of RAM, Windows 7 64-bit, MATLAB R2010a).

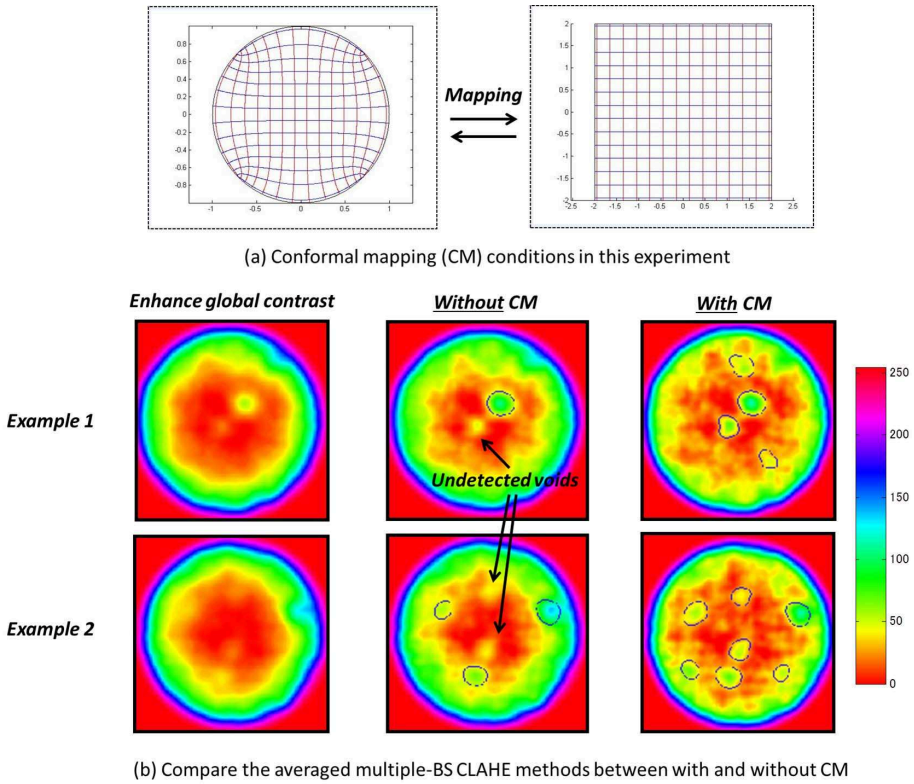

FIGURE 4. Experimental conditions and results

5. **Summary and Outlook.** In this paper, we developed the use of conformal mapping in local contrast enhancement for the circular ROI case and the practical application of improving standard BGA-void defect inspection was given as an example.

However, apart from the standard X-ray measurement system, there is another new technique, i.e., OVHM (Oblique Views at Highest Magnifications), which gives better observation in the different directions by rotating a detector instead of PCB (see [25] for more details). We simply emphasize here that although OVHM generates more difficult cases of non-circular ROI, because the conformal mapping grants us the flexibility to map ROI to a desired shape then in practice our proposal can also be extended to solve these issues using [26, 27]; we will confirm this remark in a part of our future work.

Acknowledgment. The second author wishes to thank Prof. Dr. Mohamed M. S. Nasser for his kind assistance. The second author is partially supported by the Malaysian Ministry of Education (MOE) through the Research Management Centre (RMC), Universiti Teknologi Malaysia, PSAN-UTM (Vot: Q.J090000.3200.00D28) and FRGS (Vot: R.J130000.7809.4F637).

REFERENCES

[1] M. Yunus, K. Srihari, J. Pitarresi and A. Primavera, Effect of voids on the reliability of BGA/CSA solder joints, *J. of Microelectronics Reliability*, vol.43, no.12, pp.2077-2086, 2003.

[2] D. Hillman, D. Adams, T. Pearson, B. Williams, B. Petrick, R. Wilcoxon, D. Bernard, J. Travis, E. Krastev and V. Bastin, The last will and testament of the BGA void, *Proc. of SMTA International Conference*, 2011.

[3] A. F. Said, B. L. Bennett, L. J. Karam, A. Siah, K. Goodman and J. S. Pettinato, Automated void detection in solder balls in the presence of vias and other artifacts, *IEEE Trans. Components, Packaging and Manufacturing Technology*, vol.2, no.11, pp.1890-1901, 2012.

[4] S. H. Peng and H. Do Nam, Void defect detection in ball grid array X-ray images using a new blob filter, *J. of Zhejiang University SCIENCE C*, vol.13, no.11, pp.840-849, 2012.

[5] M. Mouri, Y. Kato, H. Yasukawa and I. Takumi, A study of using nonnegative matrix factorization to detect solder-voids from radiographic images of solder, *Proc. of the 23rd IEEE International Symposium on Industrial Electronics*, pp.1074-1079, 2014.
[6] S. Nuanprasert, S. Baba and T. Suzuki, A simple automated void defect detection for poor contrast X-ray images of BGA, *Proc. of the 3rd International Conference on Industrial Application Engineering*, Kitakyushu, Japan, 2015.
[7] S. Nuanprasert, S. Baba and T. Suzuki, An efficient method of occluded solder ball segmentation for automated BGA void defect inspection using X-ray images, *Proc. of the 41st Annual Conference of the IEEE Industrial Electronics Society*, Yokohama, Japan, pp.3308-3313, 2015.
[8] G. A. Baricco, A. M. Olivero, E. J. Rodriguez and F. G. Safar, Conformal mapping-based image processing: Theory and applications, *J. of Visual Communication and Image Representation*, vol.6, no.1, pp.35-51, 1995.
[9] Y. Wang, X. Gu, T. F. Chan, P. M. Thompson and S. Yau, Conformal slit mapping and its applications to brain surface parameterization, *Medical Image Computing and Computer-Assisted Intervention*, pp.585-593, 2008.
[10] J. Shi, P. M. Thompson and Y. Wang, Human brain mapping with conformal geometry and multivariate tensor-based morphometry, *Multimodal Brain Image Analysis*, pp.126-134, 2011.
[11] A. W. K. Sangawi, A. H. M. Murid and K. W. Lee, Circular, parallel and radial slits maps and their inverses of bounded multiply connected regions with GUI, *Proc. of the 3rd International Conference on Computer Engineering & Mathematical Sciences*, Langkawi, Malaysia, pp.1-12, 2014.
[12] A. A. M. Yunus, A. H. M. Murid and M. M. S. Nasser, Numerical conformal mapping and its inverse of unbounded multiply connected regions onto logarithmic spiral slit regions and straight slit regions, *Proc. of the Royal Society of London A: Mathematical, Physical and Engineering Sciences*, vol.470, no.2162, 2014.
[13] P. Henrici, *Applied and Computational Complex Analysis, Volume 3*, Wiley and Son, New York, 1986.
[14] K. Amano, A charge simulation method for the numerical conformal mapping of interior, exterior and doubly-connected domains, *J. of Computational and Applied Mathematics*, vol.53, no.3, pp.353-370, 1994.
[15] M. R. M. Razali, M. Z. Nashed and A. H. M. Murid, Numerical conformal mapping via the Bergman kernel, *J. of Computational and Applied Mathematics*, vol.82, no.1, pp.333-350, 1997.
[16] N. Kerzman and M. R. Trummer, Numerical conformal mapping via the Szegö kernel, *J. of Computational and Applied Mathematics*, vol.14, no.1, pp.111-123, 1986.
[17] B. Fornberg, A numerical method for conformal mappings, *SIAM J. on Scientific and Statistical Computing*, vol.1, no.3, pp.386-400, 1980.
[18] R. Wegmann, An iterative method for conformal mapping, *J. of Computational and Applied Mathematics*, vol.14, no.1, pp.7-18, 1986.
[19] A. H. M. Murid, M. Z. Nashed and M. R. M. Razali, Numerical conformal mapping for exterior regions via the Kerzman-Stein kernel, *J. of Integral Equations and Applications*, vol.10, no.4, pp.517-532, 1998.
[20] M. M. S. Nasser and F. A. A. Al-Shihri, A fast boundary integral equation method for conformal mapping of multiply connected regions, *SIAM J. on Scientific Computing*, vol.35, no.3, pp.A1736-A1760, 2013.
[21] R. Kress, A Nyström method for boundary integral equations in domains with corners, *Numerische Matematik*, vol.58, no.1, pp.145-161, 1990.
[22] Y. Saad and M. H. Schultz, GMRES: A generalized minimal residual algorithm for solving nonsymmetric linear systems, *SIAM J. on Scientific and Statistical Computing*, vol.7, no.3, pp.856-869, 1986.
[23] J. Helsing and R. Ojala, On the evaluation of layer potentials close to their source, *J. of Comput. Phys.*, vol.227, no.5, pp.2899-2921, 2008.
[24] M. M. S. Nasser, Fast solution of boundary integral equations with generalized Neumann kernel, *Electronic Trans. Numerical Analysis*, vol.44, pp.189-229, 2015.
[25] GE Inspection Technologies, LP., *Solder Joint Inspection and Analysis (PCBA Brochure)*, https://www.gemeasurement.com/inspection-ndt/radiography-and-computed-tomography/phoenix-microtex, 2011.
[26] M. M. S. Nasser, A nonlinear integral equation for numerical conformal mapping, *Advances in Pure and Applied Mathematics*, vol.1, no.1, pp.47-63, 2010.
[27] K. W. Lee, A. H. M. Murid and S. H. Yeak, Conformal mapping and periodic cubic spline interpolation, *Matematika*, vol.30, no.1a, pp.8-20, 2014.